

1
2
3
4
5
6
7
8
9
10
11
12
13
14
15
16
17
18
19
20
21
22
23
24
25
26
27
28
29
30
31
32
33
34
35
36
37
38
39
40
41
42
43
44
45

**GEOLOGICAL STRUCTURE OF THE NORTHERN EASTERN
BLACK SEA FROM REGIONAL SEISMIC REFLECTION
DATA, INCLUDING THE DOBRE-2 CDP PROFILE**

by

Sydorenko, G.¹, Stephenson, R.², Yegorova, T.³, Starostenko, V.³, Tolkunov, A.¹,
Janik, T.⁴, Majdanski, M.⁴, Voitsitskiy, Z.¹, Rusakov, O.³ & Omelchenko, V.³

¹ *Technology Center of State Geophysical Company "Ukrgeofizika", Kiev, Ukraine*
² *School of Geosciences, Geology and Petroleum Geology, Meston Building, King's College,
University of Aberdeen, Aberdeen AB24 3UE, Scotland*
³ *Institute of Geophysics, National Academy of Sciences of Ukraine, Pr. Palladina 32, Kiev
03680, Ukraine*
⁴ *Institute of Geophysics, Polish Academy of Sciences, Ks. Janusza 64, 01-452 Warsaw, Poland*

46 **Abstract**

47 The margin of the northeastern Black Sea is formed by the Crimea and Kerch peninsulas
48 separating it from the Azov Sea to the north. The age and architecture of the sedimentary
49 successions in this area are described from exploration reflection seismic profiling acquired in
50 the area as well as the “one-off” regional DOBRE-2 CDP profile acquired in 2007. The
51 sediments range in age from Mesozoic to Quaternary and can be divided into five “seismo-
52 stratigraphic” complexes linked to the tectono-sedimentological evolution of the area. The
53 present regional basin architecture consists of a series of basement structural highs separating
54 a series of sedimentary depocentres and is mainly a consequence of the compressional tectonic
55 regime affecting the area since the Eocene and which has focused shortening deformation and
56 uplift along the axis of the Crimea-Caucasus inversion zone on the Kerch Peninsula and Kerch
57 Shelf of the Black Sea. Two major sedimentary basins that mainly formed during this time –
58 the Sorokin Trough in the Black Sea and the Indolo-Kuban Trough to the north of the Kerch
59 Peninsula in the Azov Sea – formed as marginal troughs to the main inversion zone.

60

61 *Keywords:* Crimean Mountains, Greater Caucasus Mountains, East Black Sea Basin, Azov
62 Sea, seismic reflection profiles, inversion tectonics, sedimentary basin formation

63

64

65 This paper focuses on the subsurface geology of the northeastern part of the Black Sea (Fig.
66 1), in particular its regional architecture of basin depocentres and basement ridges. The margin
67 of the northeastern Black Sea is formed by the Crimea and Kerch peninsulas separating it from
68 the Azov Sea to the north.

69

70 The Black Sea as a whole consists of a roughly east-west orientated depression, mainly formed
71 in the Cretaceous in the hinterland of the Pontide magmatic arc due to subduction of
72 Neotethyan lithosphere below the southern Eurasian continental margin (Dercourt *et al.* 1993;
73 Okay *et al.* 1994; Robinson & Kerusov 1997; Nikishin *et al.* 2003; Stephenson & Schellart
74 2010). At present the Black Sea is underlain by a flat, approximately 2 km deep, abyssal plain
75 that obscures two separate large depressions called the West and East Black Sea (WBS and
76 EBS) basins. These overlie crustal basement of uncertain composition and tectonic age and
77 structure and are filled with up to 14 km of Mesozoic and Cenozoic sediments (Graham *et al.*
78 2013; Nikishin *et al.* 2015a,b). The WBS and EBS basins are separated by a Mid-Black Sea

79 Ridge (MBSR), the northernmost component of which is the Andrusov Ridge, as seen in
80 Figure 1.

81

82 The Crimean Mountains, on the southern margin of the Crimea Peninsula, is the main onshore
83 expression of the Crimea-Greater Caucasus orogenic belt in the northeastern Black Sea study
84 area, running eastwards into southern Russia and Georgia. The contiguous offshore part of the
85 orogen in the present study area is referred to here as the Crimea-Caucasus inversion zone
86 (Fig. 1). It retains the memory of Mesozoic-Early Palaeogene extension as well as Eocene to
87 Miocene contraction of the lithosphere, effected mainly by thrusting. The greater regional
88 tectonic setting of the study area is described in accompanying papers in this volume (e.g.
89 Gobarenko *et al.* this volume; Starostenko *et al.* this volume).

90

91 The regional geological structure of the Black Sea has been under investigation since the
92 1980s when regional seismic lines for the entire area were published (Tugolesov *et al.* 1985;
93 Finetti *et al.* 1988; Belousov & Volvovsky 1989). More recent seismic data acquired in the
94 EBS and adjacent areas have been published by Robinson *et al.* (1996), Afanasenkov *et al.*
95 (2007), Shillington *et al.* (2008), Rangin *et al.* (2002), Khriachtchevskaia *et al.* (2010), Stovba
96 *et al.* (2009), Nikishin *et al.* (2010), Mityukov *et al.* (2012), Almendinger *et al.* (2011),
97 TPAO/BP Eastern Black Sea Project Study Group (1997), Gozhyk *et al.* (2010) and Graham *et al.*
98 (2013). A set of long regional deep seismic lines acquired in 2011 in the framework of the
99 international project “Geology Without Limits” allowed a new map of acoustic basement for
100 the whole Black Sea to be proposed (e.g. Nikishin *et al.* 2015a,b).

101

102 Marine seismic reflection surveys within the present study area were first done before the end
103 of the last century. Among the first regional 2D seismic surveys in the area were the Western
104 Geophysical (1994) and Polar Trade Research Associates (2005) surveys (Fig. 1; right-hand
105 panel). A successful exploratory well was drilled on the Subbotina anticline structure,
106 followed up by additional wells (Fig. 1; right-hand panel) and the more detailed 3D CDP Titul
107 survey undertaken by Ukrgeofizika in 2008 (Fig. 1; right-hand panel). The focus of the present
108 study is on the area lying to the south of Kerch Peninsula within the Kerch Shelf, Sorokin
109 Trough, North Black Sea High, Shatsky Ridge and East Black Sea Basin (Fig. 1).

110

111 The wide-angle refraction and reflection (WARR) profile DOBRE-2 (Starostenko *et al.* this
112 volume), utilizing on- and offshore recordings and energy sources, was acquired in 2007 by

113 Ukrainian organizations and international partners across the Azov Sea, eastern Kerch
114 Peninsula and the eastern Black Sea. The coincident DOBRE-2 regional CDP line, crossing
115 the Azov Sea, Kerch Peninsula, and the north-eastern part of the Black Sea (Fig. 1), was
116 acquired by Ukrgeofizika (the Ukrainian national geophysical company) also in 2007. The
117 geological interpretation of the DOBRE-2 CDP data are presented here, carried out in the
118 context of other seismic reflection profiling in the area and its ties to wells. The results
119 illuminate the structural relationships and ages of extensional and subsequent basin inversion
120 tectonic events as well as the 2D geometry of basement displacement associated with post-
121 Eocene inversion in this key segment of the Crimea-Caucasus deformation belt. Further, the
122 complete DOBRE-2 CDP profile (including its Kerch Peninsula and Azov Ridge segments) is
123 briefly examined in view of the presented results to examine the structural style of the
124 Crimean-Caucasus inversion zone as a whole and its associated sedimentary basins.

125

126 **Geological setting**

127

128 Rifting is the major (first-order) geodynamic process responsible for the tectonic evolution of
129 the Black Sea basins, related to closure of the Tethys and Neotethys oceans (Zonenshain & Le
130 Pichon 1986; Letouzey *et al.* 1977; Görür 1988; Okay *et al.* 1994; Robinson *et al.* 1996;
131 Nikishin *et al.* 2003; Stephenson & Schellart 2010). However, the timing of opening of the
132 Black Sea basins (i.e., the age of the oldest sediments) remains controversial. A Cretaceous
133 age was inferred from onshore geological observations by Adamia *et al.* (1974), Letouzey *et*
134 *al.* (1977), Görür (1988) and Nikishin *et al.* (2003). An Early Cretaceous to Palaeocene
135 opening was deduced by Finetti *et al.* (1988) from extensive seismic reflection data,
136 corresponding with the concepts of Zonenshain & Le Pichon (1986) and Robinson *et al.*
137 (1996). Stephenson & Schellart (2010) suggested that there was a single stage opening of
138 Black Sea as a back-arc basin resulting from asymmetric slab roll-back. Nikishin *et al.*
139 (2015b) concluded that continental rifting manifested itself from the Late Barremian to the
140 Albian, while the age of opening of the deepest basins with (sub-) oceanic crust was from
141 Cenomanian until mid-Santonian.

142

143 At present the Black Sea is undergoing compressional deformation that has been active since
144 the Eocene (Saintot *et al.* 2006b; Khriachtchevskaia *et al.* 2010; Stovba & Khriachtchevskaia
145 2011), or possibly Palaeocene (Sheremet *et al.* this volume), related to convergence of the
146 Eurasian and Afro-Arabian plates, seen, for example, as underthrusting of the Black Sea crust

147 below the crust of the Scythian platform of the Crimean and Kerch-Taman peninsulas
148 (Gobarenko *et al.* this volume).
149
150 The Crimean Mountains can be considered as the western prolongation of the Greater
151 Caucasus orogen. It is widely associated with strongly deformed Upper Jurassic-Lower
152 Cretaceous sedimentary strata, which are overlain by thin Cenozoic sediments (Kruglov &
153 Tsypko 1988). Popadyuk (2013) reported an Albian age for these strata (which they assigned
154 to the Tauric Group), which compares with recent nannofossil dating of them in the eastern
155 Crimean Mountains reported by Sheremet *et al.* (this volume). These flysch series are
156 characterized by detrital deposits, turbidites and large olistostromes containing blocks of
157 different sizes and ages. The presence of substantial volcanic ash reported by Sheremet *et al.*
158 (this volume) suggests their deposition at the same time as Early Cretaceous volcanic activity
159 in the area, which is supported the radiometric dating of Meijers *et al.* (2010) in eastern
160 Crimea and Nikishin *et al.* (2013) in western Crimea.

161
162 The DOBRE-2 CDP profile is located in the transition from the subdued offshore part of
163 Crimean orogenic belt south of the eastern Crimea Peninsula to the EBS Basin, crossing
164 numerous thrust and thrust-related folds and syn-compressional sedimentary depocentres.
165 These include the Sorokin Trough and associated positive structures, such as the Tetyaev
166 Uplift, the North Black Sea High and the Shatsky and Andrusov ridges (Fig. 1). The last two
167 form the northeastern and southwestern margins respectively of the parallel EBS Basin, which
168 is filled with Cretaceous and younger sediments as thick as 14 km that overlie a high-velocity
169 crystalline crustal layer with Moho lying at a depth of 20-24 km (Starostenko *et al.* 2004; Scott
170 *et al.* 2009; Shillington *et al.* 2009; Yegorova *et al.* 2010, 2013). The Andrusov Ridge is part
171 of the Mid-Black Sea Ridge, which is underlain by continental crust as thick as 28-29 km (e.g.
172 Shillington *et al.* 2009; Yegorova *et al.* 2010).

173
174 The study area is known to host significant oil and gas potential (e.g. Pobedash 2006; Stovba
175 *et al.* 2009). The most important discoveries in this regard are related to compressional
176 structures in an area referred to as the Kerch-Taman Trough immediately south of the Kerch
177 Strait (cf. Nikishin *et al.* this volume), the inlet to the Azov Sea from the Black Sea between
178 the Kerch and Taman peninsulas.

179

180 **Regional basin architecture in the northern eastern Black Sea from seismic reflection**
181 **profiling**

182

183 *CDP seismic dataset: acquisition and processing*

184

185 Regional investigations of the Ukrainian sector of the northeastern Black Sea have been
186 carried out using a vast set of regional seismic reflection profiles (~10000 km), including those
187 acquired by Western Geophysical in 1994 and by Polar Trade Research Associates in 2005.
188 These data, augmented by Ukrgeofizika data acquired in 2007 (DOBRE-2) and 2008 (Titul),
189 form the basis of the present paper. The location and distribution of these datasets are shown
190 in Fig. 1 (right-hand panel) with the specific profiles reproduced in this paper highlighted
191 accordingly. The main acquisition and processing parameters for the utilized seismic surveys
192 are listed in Table 1.

193

194 *Stratigraphic correlation*

195

196 Onshore seismic reflection surveys for hydrocarbon exploration were carried out on the Kerch
197 Peninsula since the middle of the 20th century and led to the discovery of a number of oil, gas
198 and gas condensate deposits in sedimentary strata of mainly Cenozoic age (cf. Fig. 1). The
199 seismic stratigraphy established onshore by Ukrgeofizika (and other Ukrainian organisations
200 such as Odesmorgeologia) was extrapolated and further developed in the offshore region
201 beginning with the 1994 Western Geophysical survey. Figure 2 shows the main seismic
202 horizons, some of which correspond to local and regional unconformities, that are readily
203 identified according to a lengthy and vast experience of seismic interpretation in the study
204 area.

205

206 Well-ties with seismic offshore are scarce in the study area except around the Subbotina
207 discovery mentioned above. Figure 3 exemplifies the geological interpreted seismic
208 stratigraphy of the area for one profile calibrated by the wells drilled on the Subbotina
209 structure. For the present study specifically, which includes the unique DOBRE-2 regional
210 CDP profile, correlation of regional reflections with stratigraphic horizons was reassessed in
211 two stages. The first of these was based on calibration with the Subbotina wells as seen in
212 Figure 3, with Subbotina-403, the discovery well and also the deepest, terminating in the
213 Lower Eocene succession. (More details of these wells and the seismic in the immediate area

214 of the Subbotina field can be found in Stovba *et al.* [2009], Gozhyk *et al.* [2010] and
215 Starostenko *et al.* [2011]). The second stage involved extrapolating the DOBRE-2 profile from
216 the (onshore) Kerch Peninsula, where the subsurface seismic stratigraphy has been well-
217 established, to the deeper part of the EBS Basin. What follows in this section is, first, a general
218 description of the established seismic stratigraphy of the study area with examples from the
219 utilized exploration datasets (Figs. 3-5; profiles located in Fig. 1) and then the Black Sea
220 segment of the DOBRE-2 regional CDP profile with a geological interpretation in this context
221 (Fig. 6).

222

223 *Regional seismo-stratigraphic complexes*

224

225 The seismic stratigraphy of the northern EBS area has conventionally been subdivided into
226 seven main “seismo-stratigraphic complexes” (e.g. Gozhyk *et al.* (2011)). In the present paper,
227 a more robust subdivision of only five such complexes is considered: a Mesozoic complex, a
228 Palaeocene-Eocene complex; the Maykopian succession of Oligocene and Early Miocene age;
229 a Middle and Upper Miocene complex and a Pliocene-Quaternary succession. These are based
230 primarily on the work of Pobedash (2008), which utilised the stratigraphy results of the
231 Subbotina-403 well (cf. Fig. 1), as well as those of Popadyuk (2009).

232

233 The Mesozoic seismo-stratigraphic complex is characterized by low-grade (weak) reflections
234 on the seismic sections in this area. The top of this complex is horizon III_m (Fig. 2), which is
235 expressed clearly on the Andrusov and Shatsky ridges and in the intervening EBS Basin (e.g.
236 Fig. 6). It is generally an erosional surface on the top of Mesozoic strata. It is difficult to
237 identify within the Sorokin Trough (e.g. Fig. 4) probably because of its high dip angle
238 conformable with overlying Cenozoic sediments. The relatively chaotic nature of reflectivity
239 within the the Mesozoic strata underlying III_m (e.g. Figs. 4, 5) is likely related to faulting of
240 probable Cretaceous age associated, for example, with Black Sea rifting. The age of
241 underlying Mesozoic strata, below horizon III_m, varies from place to place, which complicates
242 the seismic stratification and the erosional gap may be considerable.

243

244 The Palaeocene-Eocene seismo-stratigraphic complex lies between horizons III_m and II_a. The
245 Subbotina-403 well penetrated the Eocene succession, which consist mainly of marl with
246 interlayers of clay. This complex displays good dynamic reflections in the time sections. In
247 general, the sediments of this complex occur in troughs and depressions of the northern EBS

248 area (e.g. Figs. 5, 6) and it may be partly (e.g. Fig. 3) or wholly missing in places such as
249 across the North Black Sea High (Fig. 4). The complex may be present within the Sorokin
250 Trough but the overlying horizon IIa is not clearly identifiable, for example, on seismic line
251 161-94 (Fig. 4).

252

253 The Maykopian seismo-stratigraphic complex (Oligocene-Lower Miocene), lying between
254 seismic horizons Ia and IIa, is characterized by reflections of variable amplitude. According to
255 the Subbotina-403 well lithostratigraphy, the Lower Miocene succession is represented by clay
256 with siltstone interlayers, with some sandstone layers near its base, and the Oligocene
257 succession is represented mainly by clay and, towards its base, by clay with interlayered
258 siltstones and sandstones. Hydrocarbons are found in some of sand units. In the Sorokin
259 Trough the Maykopian complex is tectonically folded (e.g. Figs. 4, 6). Within the EBS Basin
260 it conformably repeats the structural forms of the Mesozoic complex with gradual flattening
261 (Figs. 4, 5) and covers the positive structures within the basin (e.g. North Black Sea High,
262 Shatsky and Andrusov ridges; Figs. 4-6) as well as the troughs as the basin subsides as a
263 whole. It is noted that the thickness of the Maykopian complex in the present interpretation
264 (e.g. Fig. 6) is much thicker over the EBS Basin and Andrusov Ridge than is other recent
265 interpretations (e.g. Stovba *et al.* 2013; Nikishin *et al.* 2015a,b; Nikishin *et al.*, this volume).
266 This is because the present interpretation was made prior to release of information from the
267 Sinop-1 well drilled on the Andrusov Ridge in Turkish territory (located in Fig. 1) and,
268 accordingly, was based on extrapolation from the Subbotina wells and other correlation points
269 on and near the Ukrainian Black Sea margin.

270

271 The Middle-Upper Miocene seismo-stratigraphic complex lies between seismic horizons Ip
272 and Ia. The latter, basal, horizon has no obvious signs of unconformity but can be associated
273 with a change in how the amplitude dynamics of the seismic wave field is expressed. Within
274 the Subbotina field the Upper Miocene is represented by clay and the the Middle Miocene by
275 clay with marl interbeds of the Tortonian age. Horizon Ip, marking the top of this complex and
276 the end of the Miocene, is an erosional surface (e.g. Figs. 3, 4).

277

278 The Pliocene-Quaternary seismo-stratigraphic complex is composed mainly of terrigenous
279 sediments. It is supposed that the component clastic materials were transported into the basin
280 by the predecessors of the modern Don, Kuban and other rivers.

281

282 *Geological interpretation of the DOBRE-2 CDP profile in the northern eastern Black Sea*
283 *(Figure 6)*

284

285 The Black Sea segment of the DOBRE-2 CDP profile shown in Figure 6 provides a regional
286 scale image of the geological structure of the main study area. A brief description follows,
287 highlighting the main diagnostic features of the geological structures – depocentres and
288 structural highs – traversed along it. Much of the detailed structural complexity associated
289 with the Cenozoic compressional tectonic stage, including mud diapirism, is obscured at the
290 scale of interpretation and, in turn, much of the Mesozoic extensional tectonic structures are
291 obscured by the later shortening processes. It is beyond the scope of the current paper to go
292 into details that may be relevant to specific hydrocarbon exploration targets, including
293 lithologies that could represent source rocks, traps or reservoirs and associated structures. The
294 main focus is on the regional-scale relationships between structural highs and depocentres and
295 the relative ages of each.

296

297 The northernmost part of the DOBRE-2 CDP profile (Fig. 6) images the submerged (below
298 sea level) southernmost part of the Crimean-Caucasus foldbelt, which is complicated by fault
299 tectonics and volcanic activity (e.g. Meijers *et al.* 2010). Jurassic- Lower Cretaceous
300 complexes can be identified in the seismic section, partly on the basis of correlation with
301 subsurface data from the southernmost part of Kerch Peninsula and partly on gravity coring in
302 the Black Sea (e.g. Tsiokha *et al.* 2008). Immediately south of the inversion zone, the profile
303 crosses what is referred to as the Kerch Shelf, which, being composed of strongly block-
304 faulted Jurassic and Cretaceous sedimentary strata, is geologically very similar to the inversion
305 zone itself. The Jurassic and Cretaceous successions are as thick as at least 2500 m and more
306 than 700 m, respectively, and show the presence of an anticlinal structure that has been
307 eroded. The southern flank of the anticline is separated from its axis by a reverse fault. The
308 Upper Jurassic sediments here are deformed by a series of low-amplitude faults in small folds.
309 Cretaceous, Palaeocene-Eocene and Maykopian strata are missing because of erosion.
310 Erosional surfaces are indeed typically found within the Oligocene-Miocene succession of the
311 Kerch Shelf. The strata on the shelf, along a system of faults affecting basement and the
312 Mesozoic succession, are dipping southwards towards the Sorokin Trough. The transition from
313 the shelf to the Sorokin Trough occurs along a fault with some 2500 m displacement. The
314 interpretation shown indicates that there is normal displacement on this fault (e.g. offset of
315 what is interpreted as horizon III_m), in which case it was formed initially during Black Sea

316 rifting and has been inverted during the later Cenozoic compressional phase of tectonics
317 although this cannot be documented at the scale of the image.

318

319 The Sorokin Trough is filled mainly with Maykopian sediments (Oligocene-Lower Miocene)
320 and, in this respect, differs significantly in structure and seismic appearance to the Kerch Shelf
321 to the north and the North Black Sea High to the south. The Sorokin Trough formed at the
322 beginning of the Oligocene and is filled with up to 5250 m of clay-rich Maykopian sediments,
323 overlain by Middle Miocene and younger strata, these being dominated by alluvial fan
324 deposits. Seismic horizon IIa, which marks the base of the Maykopian complex, is observed as
325 deep as 6.5 s (~8300 m depth) at the deepest point of the Sorokin Trough but cannot be
326 identified with confidence on the northern flank of the trough, which is structurally very
327 complex and is also affected locally by mud diapirism. Maykopian strata in the north-western
328 part of the trough form rather high-amplitude thrust-related folds that display a clear southern
329 vergence on the southern margin of the Trough along the DOBRE-2 profile.

330

331 On its southwestern margin the Sorokin Trough adjoins the North Black Sea High (and
332 contiguous Shatsky Ridge). The southern flank of the North Black Sea High, in turn, adjoins
333 the EBS Basin through a zone in which the Cretaceous and older strata are highly faulted. A
334 notable feature of the North Black Sea High (also seen well in Fig. 4) is the antiformal
335 structure composed of Mesozoic rocks as thick as 1500 m in its core. Numerous normal and
336 reverse faults affect the Mesozoic strata on the southern flank of the North Black Sea High-
337 Shatsky Ridge positive structure but faulting does not define the Palaeocene-Eocene (and, in
338 part, the Oligocene) depocentre of the adjacent EBS Basin. Stratal horizons of the EBS Basin
339 onlap the interpreted III_m horizon (top Mesozoic) on both its flanks, less steeply on the
340 northern margin with the Shatsky Ridge-North Black Sea High than the southern margin with
341 the Andrusov Ridge. According to the interpretation seen in Figure 6, the maximum depth to
342 the base Cretaceous (horizon IV) in the EBS Basin is located at a depth of ~11650 m.

343

344 The DOBRE-2 CDP profile terminates on the Andrusov Ridge, which is part of the Mid-Black
345 Sea Ridge that separates the WBS and EBS basins. The positive structure of Andrusov Ridge
346 is distinguished on the basis of seismic reflection horizon III_m, which defines a wide arch.
347 Cretaceous as well as Upper and Middle Jurassic units have been inferred in the Mesozoic
348 strata on Andrusov Ridge according to patterns seen in the reflection section (e.g. stratal
349 terminations, erosional truncations and other features; Tsiokha *et al.* 2008).

350

351 **The DOBRE-2 CDP profile as a whole**

352

353 The main focus of this paper is the regional basin architecture of the northeastern EBS,
354 coincident with the southern margin of the Crimea-Caucasus inversion zone and south of it,
355 where it has been imaged by the Black Sea segment of the DOBRE-2 regional CDP profile. It
356 is nevertheless instructive to consider this in the context of the basin architecture imaged by
357 the rest of the DOBRE-2 CDP profile and the coincident DOBRE-2 WARR profile.

358

359 Figure 7 shows in its upper panel a compressed version of the DOBRE-2 CDP profile (the
360 segment displayed in Figure 6 as well as segments acquired onshore the Kerch Peninsula and
361 offshore in the Azov Sea). The main features to be seen in the basin architecture below the
362 Kerch Peninsula and Azov Sea segments include a marked asymmetry of the Crimea-
363 Caucasus inversion zone, with a much thicker Maykopian complex on the northern margin of
364 the inversion zone than on the south. This in turn overlies a succession interpreted to be
365 Cretaceous that is much thicker than on the southern margin of the inversion zone. This major
366 sedimentary depocentre is called the Indolo-Kuban Trough and lies essentially conformably on
367 Jurassic basement that shallows rapidly to the north. Further north is a series of partially
368 inverted half grabens containing Mesozoic and Palaeogene strata called the North Azov
369 Trough. The zone of shallower basement between the Indolo-Kuban Trough is the Middle
370 Azov Uplift, where basement is shallowing, and the Azov Ridge, where the basement surface
371 is more or less flat.

372

373 The lower panel of Figure 7 displays the WARR velocity model of Starostenko *et al.* (this
374 volume) converted to two-way travel-time and displayed at the same scale as the CDP profile
375 above it. In general in the WARR model velocities in the range 1.8-4.5 km/s can be considered
376 to represent relatively undisturbed sedimentary rocks while velocities above this but less than
377 ~5.8 km/s may also represent sedimentary strata though deeply buried and highly indurated,
378 including carbonates such as those representing the Upper Jurassic succession in study area
379 (e.g. Nikishin *et al.* 2015a). Higher velocities almost certainly represent crystalline basement
380 (cf. Starostenko *et al.* this volume). No exact correspondence of velocity-seismic boundaries is
381 expected, of course, since the CDP method delineates clearly horizontal or gently inclined
382 reflectors while the WARR method can recognize near vertical discontinuities due to the
383 refraction of a wavefront.

384

385 Key seismic horizons taken from the DOBRE-2 CDP profile (upper panel; Fig. 7) are
386 superimposed on the time-converted WARR velocity model (lower panel; Fig. 7). The yellow
387 line corresponds to seismic horizon Ia (top Maykopian), the pinkish line to III_m (top
388 Mesozoic). The dotted white line represents the base of anything in the seismic image that
389 looks “sedimentary”. It corresponds roughly with the bottom of the coloured in parts of the
390 CDP image. According to the WARR velocity model anything that is below the top of the pink
391 layer (i.e., velocity > ~5.8 km/s) likely corresponds to crystalline basement rocks whereas the
392 overlying orange layer (velocity ~5.4-5.7 km/s and lying largely below the dotted white line
393 marking the base of sedimentary strata from the CDP image) could be interpreted as
394 representing highly indurated (meta-)sedimentary rocks.

395

396 Figure 7 (lower panel) indicates that the structural high below the main Crimea-Caucasus
397 inversion on the southern Kerch Peninsula and Kerch Shelf, where older sedimentary strata,
398 including Mesozoic strata occur at or near the surface, is supported by a deeper crystalline
399 basement high. The same is true of the North Black Sea High-Shatsky Ridge positive
400 structure. On the northern flank of the inversion zone, where the Maykopian succession is
401 thicker than on the southern flank and overlies a Cretaceous succession thicker than elsewhere
402 on the entire profile, the WARR velocities suggest the existence of a substantial pre-
403 Cretaceous sedimentary succession, the base of which lies at a depth greater than 20 km
404 (Starostenko *et al.* this volume).

405

406 **Discussion**

407

408 In the northeastern Black Sea the Crimea-Caucasus Inversion Zone is bordered on its southern
409 flank by a basin – the Sorokin Trough, which is in turn bordered by a basement high – the
410 North Black Sea High-Shatsky Ridge, then another depocentre – the EBS, and the another
411 basement high – the Andrusov Ridge. The Sorokin Trough is mainly filled with Maykopian
412 sediments but is structurally complicated by reverse faulting, some faults displaying
413 geometries suggesting that they are inverted extensional structures. To the north of the
414 Crimea-Caucasus Inversion Zone, as seen in the whole DOBRE-2 CDP image, the Indolo-
415 Kuban Trough is also primarily filled with Maykopian strata, although the Indolo-Kuban
416 Trough is much less structurally complex than the somewhat symmetric Sorokin Trough on the
417 southern side of the inversion zone. The younger (post-Mesozoic) sedimentary complexes are

418 mostly absent in the inversion zone itself where Mesozoic strata are near the surface,
419 structurally equivalent to the Cretaceous-Jurassic strata that is uplifted and exposed in the
420 Crimea Mountains to the west.

421

422 The WARR velocity model shows that the southern flank of the main inversion zone is
423 underlain by a basement uplift below the Mesozoic complex, indicating a thick-skinned,
424 basement-involved, mode of shortening. Seismic horizon III_m (top Mesozoic; pinkish line in
425 the lower panel of Figure 7) and the sub-parallel dotted white line at the base of clear
426 sedimentary layering can be taken as representations of vertical displacement of basement
427 during Cenozoic inversion. These show, despite some degree of asymmetry, that the Indolo-
428 Kuban and Sorokin troughs can be considered as marginal troughs formed synchronously and
429 adjacent to a developing central inversion zone as predicted theoretically by Hansen & Nielsen
430 (2003), who built a numerical model of the compressional shortening of a pre-existing rift
431 basin at the crustal scale. In the Hansen & Nielsen (2003) model the “marginal troughs” of
432 basin inversion axes (such as clearly expressed, for example, along the inverted Polish Basin;
433 e.g. Dadlez *et al.* 1995) form as a flexural isostatic response to crustal scale thickening and
434 concomitant density changes caused by the compressional shortening. This is not crustal
435 folding or buckling, which is an anelastic response to loading, nor is it flexural foreland basin
436 subsidence, which is caused by the regional isostatic response to surface loading of thrust
437 sheets. Nevertheless, the formation of these marginal trough basins is intrinsically linked to the
438 tectonic shortening and mountain-building processes that are occurring, as was recognised for
439 the Crimean Mountains and Sorokin Trough by Yudin (2011) and Yudin & Gerasimov (1992).

440

441 In a more regional context, the Indolo-Kuban Trough continues to the east of the present study
442 area (e.g. Fig. 1) to lie north of the Greater Caucasus Orogen in Russia (cf. Figure 1 in
443 Nikishin *et al.* [this volume], where it is labelled the West Kuban Basin). In the context of the
444 symmetry and co-genetic implications for the Indolo-Kuban Trough and Sorokin Trough
445 inferred in the present study, the Tuapse Trough, south of the Russian margin of the EBS, can
446 be considered to be the analogous marginal trough counterpart basin on southern flank of the
447 Greater Caucasus Orogen. Thus, on a regional scale, the Sorokin and Tuapse troughs form one
448 single tectonic entity to the south of the Crimea-Caucasus Inversion Zone and related to its
449 formation.

450

451 The asymmetry of the marginal Sorokin and Indolo-Kuban troughs displayed in the present
452 study area, centred on the southern Kerch Peninsula-Kerch Shelf, is likely related to an
453 initially asymmetric basement structure. There is an older deeper basin inferred by the WARR
454 velocity model to the north of the inversion directly underlying the thick Mesozoic succession
455 of the southern Indolo-Kuban Trough imaged by the CDP profile. This might well represent the
456 deeper expression of the Jurassic Greater Caucasus Basin, which is the primary entity being
457 inverted to form the Greater Caucasus orogen (e.g. Nikishin *et al.* 2010). Sheremet *et al.* (this
458 volume) and Saintot *et al.* (2006b) both mention geological evidence from Crimea for active
459 extensional tectonics and rapid basement subsidence in the Jurassic contemporaneous with the
460 main rifting phase of the Greater Caucasus Basin in the area of the present Greater Caucasus
461 orogeny (Saintot *et al.* 2006a). Accordingly, it is plausible that the Greater Caucasus Basin rift
462 basin lies buried between the Crimea Mountains and the Greater Caucasus itself where it is
463 seen in the exposed geology. In this case, then the seismic image suggests that the main
464 structure controlling inversion in the Kerch Peninsula-Kerch Shelf area could be the bounding
465 faults of the southern margin of the Greater Caucasus rift zone.

466

467 The Palaeocene-Eocene strata of the EBS Basin are not fault-bounded (e.g. Fig. 6) but rather
468 onlap the North Black Sea High-Shatsky Ridge on its north flank. The interpretation shown
469 here accordingly implies an absence of extensional/rift tectonics for this basin in the
470 Palaeogene, which had been previously argued (e.g. Finetti *et al.* 1988; Robinson *et al.* 1996).
471 The current interpretation, with its thin, albeit poorly constrained Cretaceous layer underlying
472 the Palaeogene depocentre is a conservative interpretation, made as such given the poor
473 imaging below what is confidently identified as seismic horizon III_m (top Mesozoic). It is
474 noted that Nikishin *et al.* (this volume) suggest from other, close-by, regional seismic profiles
475 that a substantial, fault-bounded, syn-rift (Black Sea phase of rifting) Cretaceous succession
476 underlies the IV (?) horizon as shown in Figure 6. This is a plausible interpretation that
477 presupposes but does not diagnostically document that the EBS Basin was formed by active
478 rifting in the Cretaceous, more or less contemporaneously with the WBS (e.g. Stephenson &
479 Schellart 2010). In either case, the Palaeogene succession as seen in Figure 6 may have formed
480 at least in part as a result of post-rift subsidence over a central EBS rift zone (i.e., as inferred
481 by Nikishin *et al.* this volume) but the lack of the more regional expression more typical of a
482 broader, overlapping thermal sag over a syn-rift axial depocentre suggests that its formation
483 has also been in part controlled by the compressional tectonics that started in the Eocene (or
484 possibly Palaeocene; Sheremet *et al.* this volume). As such, the North Black Sea High-Shatsky

485 Ridge would have formed primarily as a compressional structure during this time, not as a
486 flexural bulge (cf. Nikishin *et al.* this volume) and probably involving inversion of older
487 structures, contemporaneous with that in the main inversion zone to its north and the
488 subsidence of its marginal Sorokin Trough (cf. Stovba *et al.* 2013). In this regard it is noted
489 that the northward-dipping zone of seismicity recognized by Gobarenko *et al.* (this volume)
490 projects to beneath the North Black Sea High-Shatsky Ridge strengthening an interpretation in
491 which this positive structure is actively involved in current compressional tectonic processes
492 in the northern eastern Black Sea.

493

494 It is noted that the contrast in interpretations regarding the thickness of the Maykopian
495 succession overlying this area (e.g. the present interpretation [e.g. Fig. 6] and those of Stovba
496 *et al.* [2013] and Nikishin *et al.* [this volume]) has significance for inferring the timing of a key
497 compressional deformation event in the Cenozoic. The latter interpretations permits this to be
498 later than the former: more or less synchronous with (Oligocene-Early Miocene) Maykopian
499 deposition rather than terminated prior to the end of the Oligocene.

500

501 **Summary and conclusions**

502

503 The age and architecture of the sedimentary successions of the northeastern EBS basin have
504 been documented from reflection seismic profiling acquired in the area and investigated by
505 Ukrgeofizika and other Ukrainian organisations. These include the one-off regional DOBRE-2
506 CDP profile acquired by Ukrgeofizika in 2007. These studies have allowed the sedimentary
507 successions of the area – from the Kerch Peninsula and Kerch Shelf south to the central Black
508 Sea – to be subdivided into a number of tectono-sedimentary complexes and have revealed a
509 series of basement structural highs separating a series of sedimentary depocentres. This
510 regional architecture of the northeastern EBS was then compared to that imaged to the north of
511 the Kerch Peninsula in the Azov Sea from the regional DOBRE-2 CDP as a whole.

512

513 The dominant driver of the present-day architecture of the study area, as indicated by
514 structural and stratigraphic relationships including erosional gaps and hiatuses, folding and
515 reverse faulting, has been the compressional tectonic regime affecting the area during the
516 Cenozoic. Some but not all reverse faults can be seen to be inverted normal faults developed
517 during earlier extensional regimes when the Jurassic Greater Caucasus and Cretaceous Black
518 Sea back-arc basins were formed.

519

520 Compressional deformation and shortening is most severe in the Kerch Peninsula-Kerch Shelf
521 area, which can be characterised as the central inversion zone within the study area. It is part
522 of the contiguous Crimea-Caucasus orogenic belt that is more developed in the Crimean
523 Mountains to the west and most developed in the Greater Caucasus Orogeny to the east.

524

525 Some specific conclusions are as follows:

526

527 (1) Cenozoic sediments are as thick as 5 km in the area of the Subbotina hydrocarbon
528 discovery (part of what is called the Kerch-Taman Trough). The discovery is within an
529 anticlinal structure complicated by thrust faults unconformably overlain by Quaternary-
530 Pliocene deltaic deposits.

531

532 (2) The Sorokin Trough is some 40-50 km wide, covering the major part of Black Sea
533 continental margin, locates ~50 km south of the Crimean Peninsula coast and running for ~150
534 km along the coastline. It is filled with Maikopian sediments, predominantly) clays of greater
535 than 5 km thickness overlain with the Middle Miocene-Quaternary sandy-clay deposits as
536 thick as 3.5-4 km.

537

538 (3) The Sorokin Trough is a marginal trough to the main Crimea-Caucasus Inversion Zone
539 with the Indolo-Kuban Trough beneath the Azov Sea its northern margin counterpart in the
540 present study area.

541

542 (4) The Shatsky Ridge and the EBS Basin (Palaeocene) are at least in part syn-compressional
543 structures.

544

545 **Acknowledgements**

546

547 The authors thank the chief editor of this Special Publication, Marc Sosson (University of Nice
548 Sophia Antipolis, France) and reviewers... RS acknowledges support from the Royal Society
549 of Edinburgh for facilitating the collaboration that has led to the production of this manuscript.
550 This work was partly supported within the statutory activities No. 3841/E-41/S/2015 of the
551 Ministry of Science and Higher Education of Poland.

552

553 **References**

- 554
- 555 ADAMIA, S., GAMKRELIDZE, I. P., ZAKARIADZE, G. S. & LORDKIPANIDZE, M. V. 1974.
- 556 Adjara-Trialeti trough and the problem of the Black Sea origin. *Geotectonika*, **1**, 78-94 (in
- 557 Russian).
- 558
- 559 AFANASENKOV, A. P., NIKISHIN, A. M. & OBUKHOV, A. N. 2007. *Eastern Black Sea Basin:*
- 560 *Geological Structure and Hydrocarbon Potential*. Nauchnui Mir, Moscow (in Russian).
- 561
- 562 ALMENDINGER, O. A., MITYUKOV, A. V., MYASOEDOV, N. K. & NIKISHIN, A. M. 2011.
- 563 Modern erosion and sedimentation processes in the deep-water part of the Tuapse Trough
- 564 based on the data of 3D seismic survey. *Dokl. Earth Sci.*, **439** (Part 1), 899-901.
- 565
- 566 BELOUSOV, V. V. & VOLVOVSKY, B. S. (eds) 1989. *Structure and Evolution of the Earth's*
- 567 *Crust and Upper Mantle of the Black Sea*. Nauka, Moscow (in Russian).
- 568
- 569 DADLEZ, R., NARKIEWICZ, M., STEPHENSON, R.A., VISSER, M & VAN WEES, J-D. 1995.
- 570 Tectonic evolution of the Polish Trough: modelling implications and significance for
- 571 central European geology. *Tectonophysics*, **252**, 179-195.
- 572
- 573 DERCOURT, J., GAETANI, M. & VRIELYNCK, B. (eds) 1993. *Atlas Tethys, Palaeoenvironmental*
- 574 *Maps*. Gauthier-Villars, Paris.
- 575
- 576 FINETTI, I., BRICCHI, G., DEL BEN, A., PIPAN, M. & XUAN, Z. 1988. Geophysical study of
- 577 the Black Sea. *Bolletino di Geofisica Teorica ed Applicata*, **XXX/117-118**, 197-324.
- 578
- 579 GOBARENKO, V., YEGOROVA, T. & STEPHENSON, R., this volume. Local tomography model
- 580 of the northeast Black Sea: intraplate crustal underthrusting.
- 581
- 582 GÖRÜR, N. 1988. Timing of opening of the Black Sea Basin. *Tectonophysics*, **147**, 247-262.
- 583
- 584 GOZHYK, P. F., BAGRIY, I. D., VOITSYTSKYI, Z. YA, GLADUN, V. V., MASLUN, N. V.,
- 585 ZNAMENSKA, T. O., AKS'OM, S. D., KLIUSHYNA, G. V., IVANIK, O. M., KLOCHKO, V. P.,
- 586 MEL'NICHUK, P. M., PALIY, V. M. & TSIOKHA, O. G. 2010. *Geological-structural-thermo-*
- 587 *atmogeochemical substantiation of petroleum presence in the Azov-Black Sea Aquatory*.
- 588 Logos, Kyiv, p. 419 (in Ukrainian).
- 589
- 590 GOZHYK, P.F., MASLUN, N.V. et al. 2011. Stratigraphic Structure of Cenozoic Deposits of
- 591 Prekerch Shelf and East Black Sea Basin. AAPG, Search and Discovery Article #50395.
- 592
- 593 GRAHAM, R., KAYMAKCI, N. & HORN, B. W. 2013. The Black Sea: something different?
- 594 *GeO ExPro*. October 58-62.
- 595
- 596 HANSEN, D. L. AND NIELSEN S. B. 2003. Why rifts invert in compression. *Tectonophysics*, **373**,
- 597 5-24.
- 598
- 599 KHRIACHTCHEVSKAIA, O., STOVBA, S. & STEPHENSON, R. 2010. Cretaceous-Neogene
- 600 tectonic evolution of the northern margin of the Black Sea from seismic reflection data
- 601 and tectonic subsidence analysis. In: Sosson, M., Kaymakci, N., Stephenson, R., Bergerat,

602 F. & Starostenko V. (eds) *Sedimentary Basin Tectonics from the Black Sea and Caucasus*
603 *to the Arabian Platform*, Geological Society, London, Special Publications, **340**, 137-157.
604

605 KRUGLOV, S. S. & TSYPKO, A. K (eds.) 1988. *Tectonics of Ukraine*, Nedra, Moscow (in
606 Russian).
607

608 LETOUZEY, J., BIJOU-DUVAL, B., DORKEL, A., GONNARD, R., KRISTCHEV, K., MONTADERT,
609 L. & SUNGURLU, O. 1977. The Black Sea: a marginal basin; geophysical and geological
610 data. In: Bijou-Duval, B. & Montadert, L. (eds) *International Symposium on the*
611 *Structural History of the Mediterranean Basins*, Editions Technip, Paris, 363-376.
612

613 MEIJERS, M. J. M., VROUWE, B., VAN HINSBERGEN, D. J. J., KUIPER, K. F., WIJBRANS, J.,
614 DAVIS G. R., STEPHENSON, R. A., KAYMAKCI, N., MATENCO, L. & SAINTOT, A. 2010.
615 Jurassic arc volcanism on Crimea (Ukraine): Implications for the paleo-subduction zone
616 configuration of the Black Sea region. *Lithos*, **119**, 412-426.
617

618 MITYUKOV, A. V., NIKISHIN, A. M., ALMENDINGER, O. A., BOLOTOV, S. N., LAVRISHCHEV,
619 V. A., MYASOEDOV, N. K., RUBTSOVA, E. V. 2012. A sedimentation model of the
620 Maikop deposits of the Tuapse Basin in the Black Sea according to the results of 2-D and
621 3-D seismic surveys and field works in the Western Caucasus and Crimea. *Moscow U.*
622 *Geol. Bull.* **67** (2), 81-92.
623

624 NIKISHIN, A. M., ERSHOV, A. V. & NIKISHIN, V. A. 2010. Geological history of Western
625 Caucasus and adjacent foredeeps based on analysis of the regional balanced section. *Dokl.*
626 *Earth Sci.*, **430** (2), 155-157. <http://dx.doi.org/10.1134/S1028334X10020017>.
627

628 NIKISHIN, A. M., KOROTAEV, A. M., ERSHOV, A. V. & BRUNET, M.-F. 2003. The Black Sea
629 basin: tectonic history and Neogene-Quaternary rapid subsidence modelling, *Sedimentary*
630 *Geology*, **156**, 149-168.
631

632 NIKISHIN, A. M., KHOTYLEV, A. O., BYCHKOV, A. YU, KOPAEVICH, L. F., PETROV, E. I. &
633 YAPASKURT, V. O. 2013. Cretaceous volcanic belts and the Black Sea Basin history.
634 *Moscow U. Geol. Bull.*, **68** (3), 141-154. <http://dx.doi.org/10.3103/S0145875213030058>
635

636 NIKISHIN, A. M., OKAY, A. I., TÜYSÜZ, O., DEMIRER, A., AMELIN, N & PETROV, E. 2015a. The
637 Black Sea basins structure and history: New model based on new deep penetration
638 regional seismic data. Part 1: Basins structure and fill. *Marine and Petroleum Geology*,
639 **59**, 638-655.
640

641 NIKISHIN, A.M., OKAY, A. I., TÜYSÜZ, O., DEMIRER, A., WANNIER, M., AMELIN, N. & PETROV,
642 E. 2015b. The Black Sea basins structure and history: New model based new deep
643 penetration regional seismic data. Part 2: Tectonic history and paleogeography. *Marine*
644 *and Petroleum Geology*, **59**, 656-670.
645

646 NIKISHIN, A. M., WANNIER, M., ALEKSEEV, A. S., ALMENDINGER, O. A., FOKIN, P. A.,
647 GABDULLIN, R. R., KHUDOLEY, A. K., KOPAEVICH, L. F., MITYUKOV, A. V., PETROV, E. I.
648 & RUBTSOVA, E. V., this volume. Mesozoic to recent geological history of southern
649 Crimea and the Eastern Black Sea region.
650

- 651 OKAY, A. I., ŞENGÖR, A. M. C. & GÖRÜR, N. 1994. Kinematic history of the opening of the
652 Black Sea and its effect on the surrounding regions. *Geology*, **22**, 267-270.
653
- 654 POBEDASH, M. 2006. Forecast of oil zones in the Black Sea based on regional seismic studies
655 and synthesis of information on the geology, geodynamics and petroleum potential of the
656 Azov-Black Sea region. DGP TC “UkrGeofizika”, Kyiv (in Ukrainian).
657
- 658 POBEDASH, M. 2008. Report on regional geophysical surveys along the DOBRE-2 profile
659 (Feodosiya-Starobeshevo). Report of State Geophysical Company “UkrGeofizika”, Kyiv
660 (in Ukrainian).
661
- 662 POPADYUK, I. 2009. CDP regional seismic study within the Ukrainian sector of the Black Sea.
663 Report of the Company “Naukanaftogaz”, Kyiv (in Ukrainian).
664
- 665 POPADYUK, I. V., STOVBA S. M. & KHRIACHTCHEVSKAIA, O. I. 2013. The new geological map
666 of the Crimea Mountains by SPK-Geoservice as a new approach to understanding the
667 Black Sea Region. Abstracts, Darius Programme Workshop, 24-25 June, 2013, Tbilisi,
668 Georgia, 48-50.
669
- 670 RANGIN, C., BADER, A. G., PASCAL, G., ECEVITOĞLU, B. & GORÜR, N. 2002. Deep structure
671 of the Mid Black Sea High (offshore Turkey) imaged by multi-channel seismic survey
672 (BLACKSIS cruise). *Mar. Geol.*, **182**, 265-278.
673
- 674 ROBINSON, A.G. & KERUSOV, E. 1997. Stratigraphic and structural development of the Gulf of
675 Odessa, Ukrainian Black Sea: implications for petroleum explorations. In: Robinson, A.G.
676 (ed) *Regional and Petroleum Geology of the Black Sea and Surrounding Region*, AAPG
677 Memoir, **68**, 369-380.
678
- 679 ROBINSON, A.G., RUDAT, J.H., BANKS, C.J. & WILES, R. L. F. 1996. Petroleum geology of
680 the Black Sea. *Marine and Petroleum Geology*, **13**, 195-223.
681
- 682 SAINTOT, A., BRUNET, M.-F., YAKOVLEV, F., SÉBRIER, M., STEPHENSON, R., ERSHOV, A.,
683 CHALOT-PRAT, F. & MCCANN, T., 2006a. The Mesozoic-Cenozoic tectonic evolution of
684 the Greater Caucasus. In: Gee, D. & Stephenson, R. (eds) *European Lithosphere*
685 *Dynamics*. Geological Society, London, Memoirs, **32**, 277-289.
686
- 687 SAINTOT, A., STEPHENSON, R., STOVBA, S., BRUNET, M.-F., YEGOROVA, T. &
688 STAROSTENKO, V. 2006b. The evolution of the southern margin of the Eastern Europe
689 (Eastern European and Scythian platforms) from latest Precambrian-Early Palaeozoic to
690 the Early Cretaceous. In: Gee, D. & Stephenson, R. (eds) *European Lithosphere*
691 *Dynamics*. Geological Society, London, Memoirs, **32**, 481-505.
692
- 693 SCOTT, C. L., SHILLINGTON, D. J., MINSHUL, T. A., EDWARDS, R. A., BROWN, P. J. &
694 WHITE, N. J., 2009. Wide-angle seismic data reveal extensive overpressures in the Eastern
695 Black Sea Basin. *Geophys. J. Int.*, **178**, 1145-1163. <http://dx.doi.org/10.1111/j.1365-246X.2009.04215.x>
696
697
- 698 SHEREMET (KORNIYENKO), YE., SOSSON, M., MÜLLER, C., GINTOV, O., MUROVSKAYA, A.
699 YEGOROVA, T., this volume. Key problems of stratigraphy in the Eastern Crimea
700 Peninsula: some insights from new dating and structural data.

701
702 SHILLINGTON, D. J., WHITE, N., MINSHULL, T. A., EDWARDS, G. R. H., JONES, S.,
703 EDWARDS, R. A. & SCOTT, C. L. 2008. Cenozoic evolution of the eastern Black Sea: A
704 test of depth-dependent stretching models, *Earth planet. Sci. Lett.*, **265**, 360-378, doi:
705 10.1016/j.epsl.2007.10.033.
706
707 SHILLINGTON, D. J., SCOTT, C. L., MINSHULL, T. A., EDWARDS, R. A., BROWN, P. J. &
708 WHITE, N. 2009. Abrupt transition from magma-starved to magma-rich rifting in the
709 eastern Black Sea. *Geology*, **37**/1, 7-10.
710
711 STAROSTENKO et al., this volume. DOBRE-2 WARR profile: the Earth's crust across Crimea
712 between the pre-Azov Massif and the north eastern Black Sea Basin.
713
714 STAROSTENKO, V., BURYANOV, V., MAKARENKO, I., RUSAKOV, O., STEPHENSON, R., NIKISHIN,
715 A., GEORGIEV, G., GERASIMOV, M., DIMITRIU, R., LEGOSTAEVA, O., PCHELAROV, V. &
716 SAVA, C. 2004. Topography of the crust-mantle boundary beneath the Black Sea Basin.
717 *Tectonophysics*, **381**, 211-233.
718
719 STAROSTENKO V.I., KRUPSKIY, B.I. et al. 2011. Fault Tectonics of the NE Black Sea Shelf and
720 Its Relevance Hydrocarbon Potential. AAPG, Search and Discovery Article #30155.
721
722 STEPHENSON, R. & SCHELLART, W. P. 2010. The Black Sea back-arc basin: insights on its
723 origin from geodynamic models of modern analogues. In: Sosson, M., Kaymakci, N.,
724 Stephenson, R., Bergerat, F. & Starostenko V. (eds) *Sedimentary Basin Tectonics from the*
725 *Black Sea and Caucasus to the Arabian Platform*, Geological Society, London, Special
726 Publications, **340**, 11-21.
727
728 STOVBA, S. & KHRIACHTCHEVSKAIA, O. 2011. Driving and triggering mechanisms of inversion
729 tectonics in the Ukrainian Black Sea. In: 3rd International Symposium on the Geology of
730 the Black Sea Region, 1–10 October 2011, Bucharest, Romania, Abstracts, GeoEcoMar
731 (Suppl), 17, 177-179.
732
733 STOVBA, S., KHRIACHTCHEVSKAIA, O. & POPADYUK, I. 2009. Hydrocarbon-bearing areas in the
734 eastern part of the Ukrainian Black Sea. *Leading Edge*, **28** (9), 1042-1045
735
736 STOVBA, S., KHRIACHTCHEVSKAIA, O. & POPADYUK, I. 2013. Crimea and Ukrainian Eastern
737 Black Sea Basin as an inverted Early Cretaceous rift system. Abstracts, Darius
738 Programme Workshop, 24-25 June, 2013, Tbilisi, Georgia.
739
740 TPAO/BP EASTERN BLACK SEA PROJECT STUDY GROUP 1997. A promising area in the Eastern
741 Black Sea. *Leading Edge*, **28** (9), 1001-1004.
742
743 TSIOKHA, O., SYDORENKO, G., VOITSITSKIY, Z. & POBEDASH, M. 2008. Regional geophysical
744 research along the DOBRE-2 profile. Report of State Geophysical Company
745 "UkrGeofizika", Kyiv (in Ukrainian).
746
747 TUGOLESOV, D. A., GORSHKOV, A. S., MEISNER, L. B. et al. 1985. *Tectonics of Mesozoic-*
748 *Cenozoic Successions of the Black Sea Basin*. Nedra, Moscow (in Russian).
749

- 750 YEGOROVA, T. & GOBARENKO, V. 2010. Structure of the Earth's crust and upper mantle of
751 West- and East Black Sea Basins revealed from geophysical data and their tectonic
752 implications. In: Sosson, M., Kaymakci, N., Stephenson, R., Bergerat, F. & Starostenko
753 V. (eds) *Sedimentary Basin Tectonics from the Black Sea and Caucasus to the Arabian*
754 *Platform*, Geological Society, London, Special Publications, **340**, 23-42.
755
- 756 YEGOROVA, T. P., BARANOVA, E. P. & OMELCHENKO, V. D. 2010. The crustal structure of
757 the Black Sea from reinterpretation of Deep Seismic Sounding data acquired in the 1960s.
758 In: Sosson, M., Kaymakci, N., Stephenson, R., Bergerat, F. & Starostenko V. (eds)
759 *Sedimentary Basin Tectonics from the Black Sea and Caucasus to the Arabian Platform*,
760 Geological Society, London, Special Publications, **340**, 43-56.
761
- 762 YEGOROVA, T., GOBARENKO, V. & YANOVSKAYA, T. 2013. Lithosphere structure of the
763 Black Sea from 3-D gravity analysis and seismic tomography. *Geophys. J. Int.*, **193**, 287-
764 303.
765
- 766 YUDIN, V.V. & GERASIMOV, M.YE. 1992. Geodynamic model of the Crimea-Black Sea and
767 adjacent regions. In: *Geodynamics of the Crimea-Black Sea Region*, Simferopol, 16-23 (in
768 Russian).
769
- 770 YUDIN, V.V. 2011. *Geodynamics of Crimea*. Simferopol, DAAIPI, 336 p. (in Russian).
771
- 772 ZONENSHAIN, L. P. & LE PICHON, X. 1986. Deep basins of the Black Sea and Caspian Sea as
773 remnants of Mesozoic back-arc basins. *Tectonophysics*, **123**, 181-211.
774

777 Table 1. Acquisition parameters and basic processing sequence for CDP data within the Black Sea (Ukrainian sector) used in the present study.

777

ACQUISITION PARAMETERS			
Seismic survey	DOBRE-2 (2007) & Titul-407 (2008)	Polar Trade Research Associates (2005)	Western Geophysical (1994)
Ship's name	Iskatel	Professor Polshkov	Western Challenger
Recording system	MSX I/O	MSTS Syntrak 480-16	TITAN 1000
Recording format	SEG-D	SEG-D	SEG-D
Record length (s)	15	15	9
Sampling rate (ms)	2	2	2
Streamer type	INPUT/OUTPUT	Syntrak 480 Digital Model LDA	Streamer
Recorded seismic channels	240	480	324
Length of streamer (m)	3000	6000	4050
Group interval (m)	12.5	12.5	12.5
Minimal offset (m)	165	120	137
Cable depth (m)	9	8	9
Seismic source	Sleeve airgun array	Airgun array system	Sleeve airgun array
Total volume (cubic inches)	1520	3800	4500
Shot interval (m)	50	50	25
Source depth (m)	6	6	6
DATA PROCESSING FLOW			
Reading of the field seismic data in SEG-D format and reformat to ProMAX system			
Geometry definition and create database profile			
Interactive editing bad shots and receivers			
CDP velocity analysis			
Getting stack brute			
Amplitude recovery			
Bandpass filtering			
The weakening of linear wave noise (FK filtering)			
Predictive minimum-phase deconvolution			
Velocity analysis (step each 100 CDP)			
Suppression of multiples (Radon filtering)			
Velocity analysis (each 50 CDP step).			
Additional bottom and top muting			
DMO			
Velocity Analysis after DMO			
Final stacking			
Minimum-phase deconvolution			
FX deconvolution			
Kirchhoff post-stack migration			
Variable in time bandpass filtering			

778

779

780 **Figure captions**

781

782 **Figure 1.** The study area in the northeastern Black Sea-Crimea (Kerch Peninsula)-Azov Sea:
783 tectonic and structural background (left panel) and locations of seismic lines (55-407, 161-94,
784 54-94 and DOBRE-2; both panels) and wells (Sinop-1, Subbotina 1, 2, 3 and 403; right panel)
785 mentioned in the text. Blue contour lines (50, 100, 200, 500, 1000, 1500 and 2000 m)
786 represent bathymetry (water depths are less than 50 m everywhere in the Azov Sea) and black
787 contour lines represent the structural disposition of horizon III_m (see text), the top of the
788 Mesozoic succession (contour interval generally 200-300 m, depending on detail). The seismic
789 grids seen in the right-hand panel are those the interpretation of which has contributed to the
790 present study (Western Geophysical 1994 – black lines; Polar Trade Research Associates 2005
791 survey – turquoise lines; Ukrgeofizika Titul-407 2008 – green lines). The highlighted profiles
792 are reproduced with geological interpretations in this paper.

793

794 **Figure 2.** Ukrgeofizika regional stratigraphic column for the study area identifying seismic
795 horizons interpreted on seismic profiles seen in Figures 3-7. Not all labelled horizons or
796 unconformities are discussed in the present text.

797

798 **Figure 3.** Seismic profile 55-407 (located on Figure 1) across the Subbotina oil field, within
799 the Kerch Trough dominated by thrust tectonics and showing wells 1-3 and 403 (Fig. 1). Solid
800 black lines indicate seismo-stratigraphic horizons with labels related to the stratigraphic
801 column in Figure 2. Red lines indicate inferred thrusts.

802

803 **Figure 4.** Seismic profile 161-94 (located on Figure 1) across the Sorokin Trough and North
804 Black Sea High. Solid black lines indicate seismo-stratigraphic horizons with labels related to
805 the stratigraphic column in Figure 2. Red lines indicate inferred thrusts.

806

807 **Figure 5.** Seismic profile 54-94 (located on Figure 1) across the northern termination of the
808 EBS Basin. Solid black lines indicate seismo-stratigraphic horizons with labels related to the
809 stratigraphic column in Figure 2. Red lines indicate inferred thrusts.

810

811 **Figure 6.** Seismic profile DOBRE-2 (northern eastern Black Sea segment) from the Kerch
812 Shelf south to the Andrusov Ridge on the southern flank of the EBS Basin axis.
813 Solid black lines indicate seismo-stratigraphic horizons with labels related to the stratigraphic
814 column in Figure 2. Red lines indicate inferred faults.

815

816 **Figure 7.** Upper panel: the whole of the DOBRE-2 regional CDP profile, horizontally
817 compressed, showing the seismo-stratigraphic complexes of the Kerch Peninsula and Azov
818 Sea correlatable with those of the northern eastern Black Sea. Solid black lines indicate
819 seismo-stratigraphic horizons with labels related to the stratigraphic column in Figure 2. Red
820 lines indicate inferred faults. Lower panel: DOBRE-2 WARR velocity model over the extent
821 of the DOBRE-2 CDP profile shown in the upper panel with the vertical axis converted to
822 two-way travel-time, with key horizons from the DOBRE-2 CDP profile superimposed (as
823 explained in the text).

Table 1. Acquisition parameters and basic processing sequence for CDP data within the Black Sea (Ukrainian sector) used in the present study.

ACQUISITION PARAMETERS			
Seismic survey	DOBRE-2 (2007) & Titul-407 (2008)	Polar Trade Research Associates (2005)	Western Geophysical (1994)
Ship`s name	Iskatel	Professor Polshkov	Western Challenger
Recording system	MSX I/O	MSTS Syntrak 480-16	TITAN 1000
Recording format	SEG-D	SEG-D	SEG-D
Record length (s)	15	15	9
Sampling rate (ms)	2	2	2
Streamer type	INPUT/OUTPUT	Syntrak 480 Digital Model LDA	Streamer
Recorded seismic channels	240	480	324
Length of streamer (m)	3000	6000	4050
Group interval (m)	12.5	12.5	12.5
Minimal offset (m)	165	120	137
Cable depth (m)	9	8	9
Seismic source	Sleeve airgun array	Airgun array system	Sleeve airgun array
Total volume (cubic inches)	1520	3800	4500
Shot interval (m)	50	50	25
Source depth (m)	6	6	6
DATA PROCESSING FLOW			
Reading of the field seismic data in SEG-D format and reformat to ProMAX system			
Geometry definition and create database profile			
Interactive editing bad shots and receivers			
CDP velocity analysis			
Getting stack brute			
Amplitude recovery			
Bandpass filtering			
The weakening of linear wave noise (FK filtering)			
Predictive minimum-phase deconvolution			
Velocity analysis (step each 100 CDP)			
Suppression of multiples (Radon filtering)			
Velocity analysis (each 50 CDP step).			
Additional bottom and top muting			
DMO			
Velocity Analysis after DMO			
Final stacking			
Minimum-phase deconvolution			
FX deconvolution			
Kirchhoff post-stack migration			
Variable in time bandpass filtering			

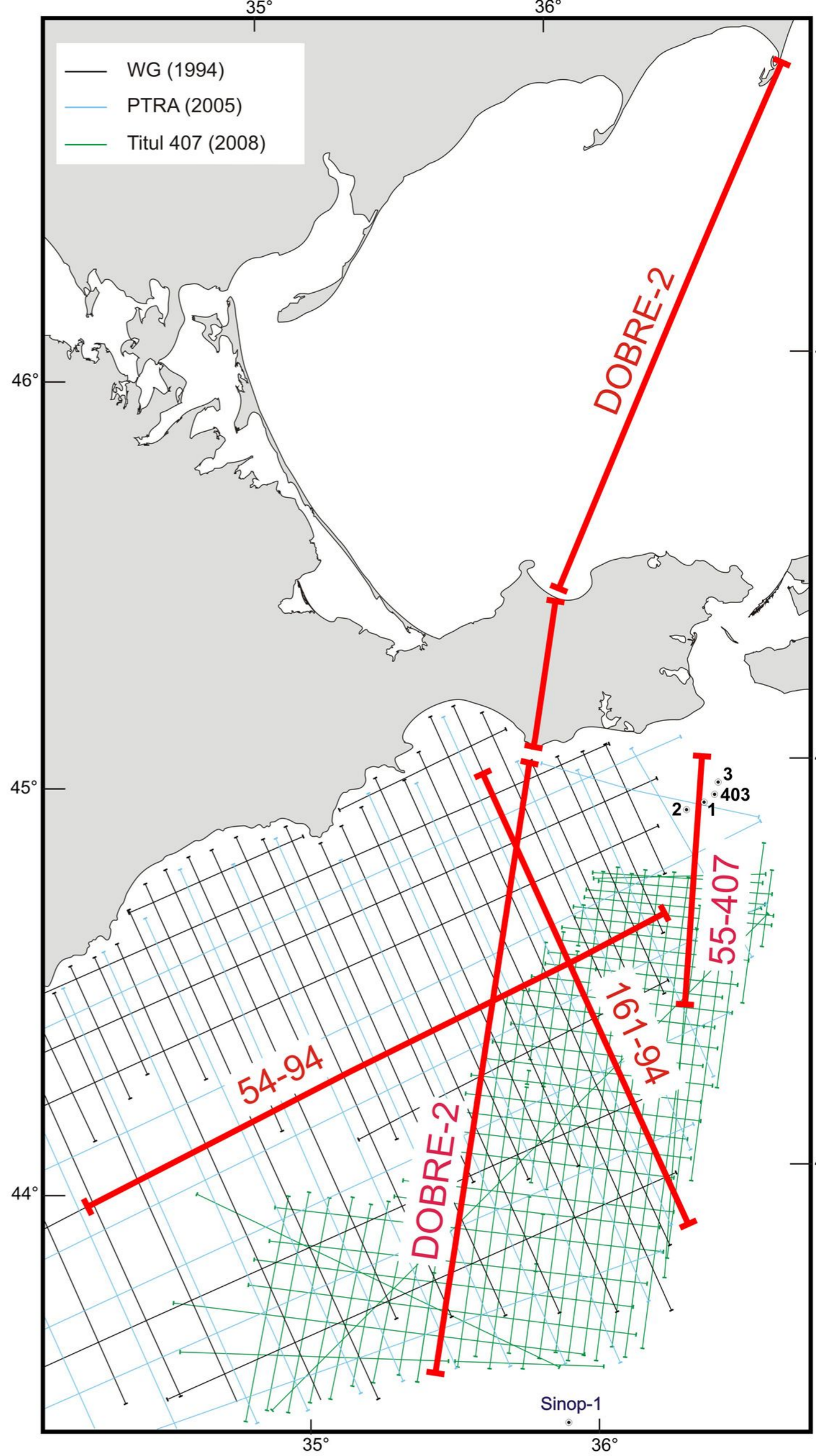


Fig. 1

Era	Period	Epoch	Stage	Unconformity	Seismic horizon	
CENOZOIC	Neogene	Pliocene	Piacenzian			
			Zanclean	Attic	Ip	
			Messinian		Is	
		Miocene	Tortonian			
			Serravallian			
			Langhian	Styrian	Ia	
			Burdigalian			
			Aquitanian	Maykopian	Ib	
			Chattian			
			Oligocene	Rupelian	Iberian	IIa
				Priabonian		
				Eocene	Bartonian	
	Lutetian				III	
	Ypresian					
	Palaeocene	Thanetian				
		Selandian				
		Danian	Laramide	IIIIm		
	Maastrichtian					
	Cretaceous	Upper	Campanian			
			Santonian			
			Coniacian			
			Turonian			
			Cenomanian			
			Lower	Albian		
				Aptian		
		Barremian				
		Hautervian				
Valanginian						
Berriasian						
Jurassic		Upper		Tithonian		IV
				Kimmeridgian		
			Oxfordian			
Middle		Callovian				
	Bathonian					
	Bajocian					
	Aalenian					

SEISMIC LINE 55-407 WITH GEOLOGICAL INTERPRETATION

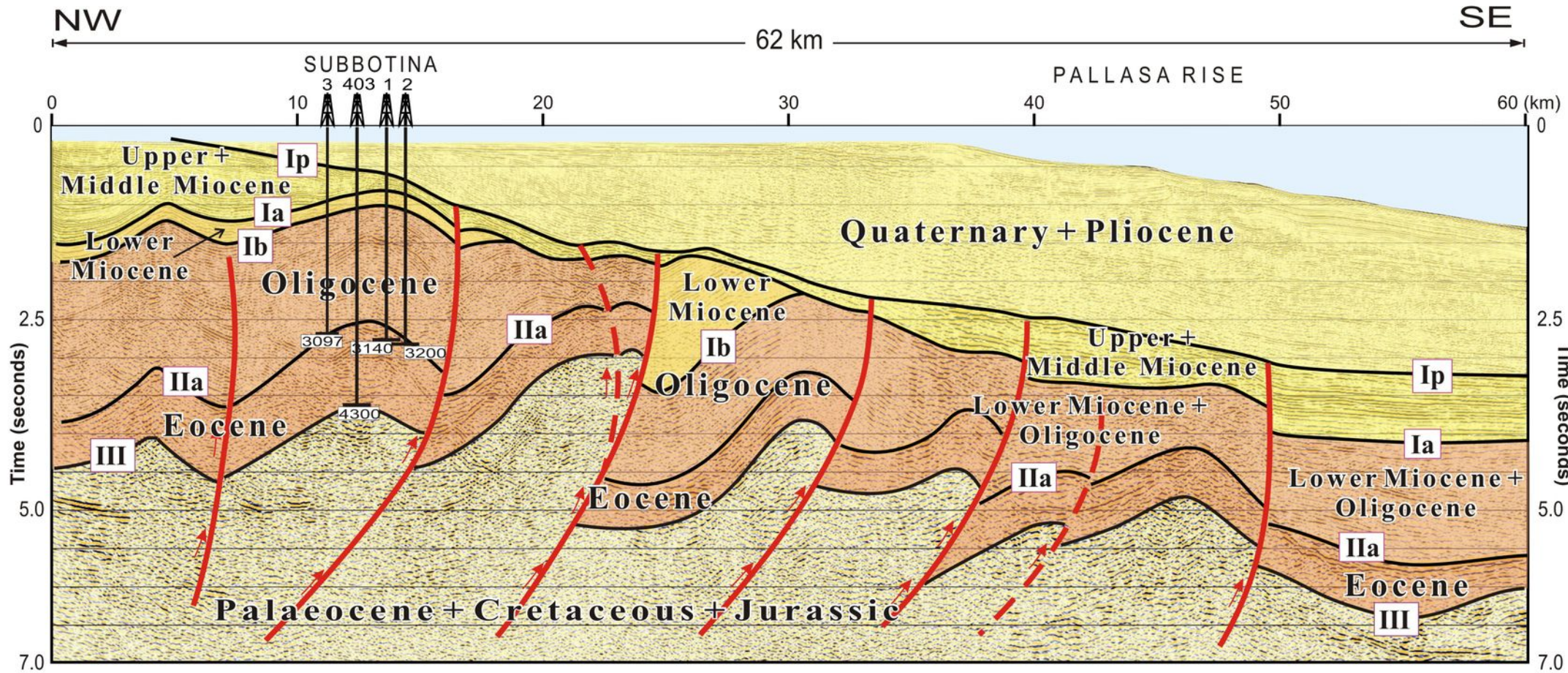


Fig. 3

SEISMIC LINE 161-94 WITH GEOLOGICAL INTERPRETATION

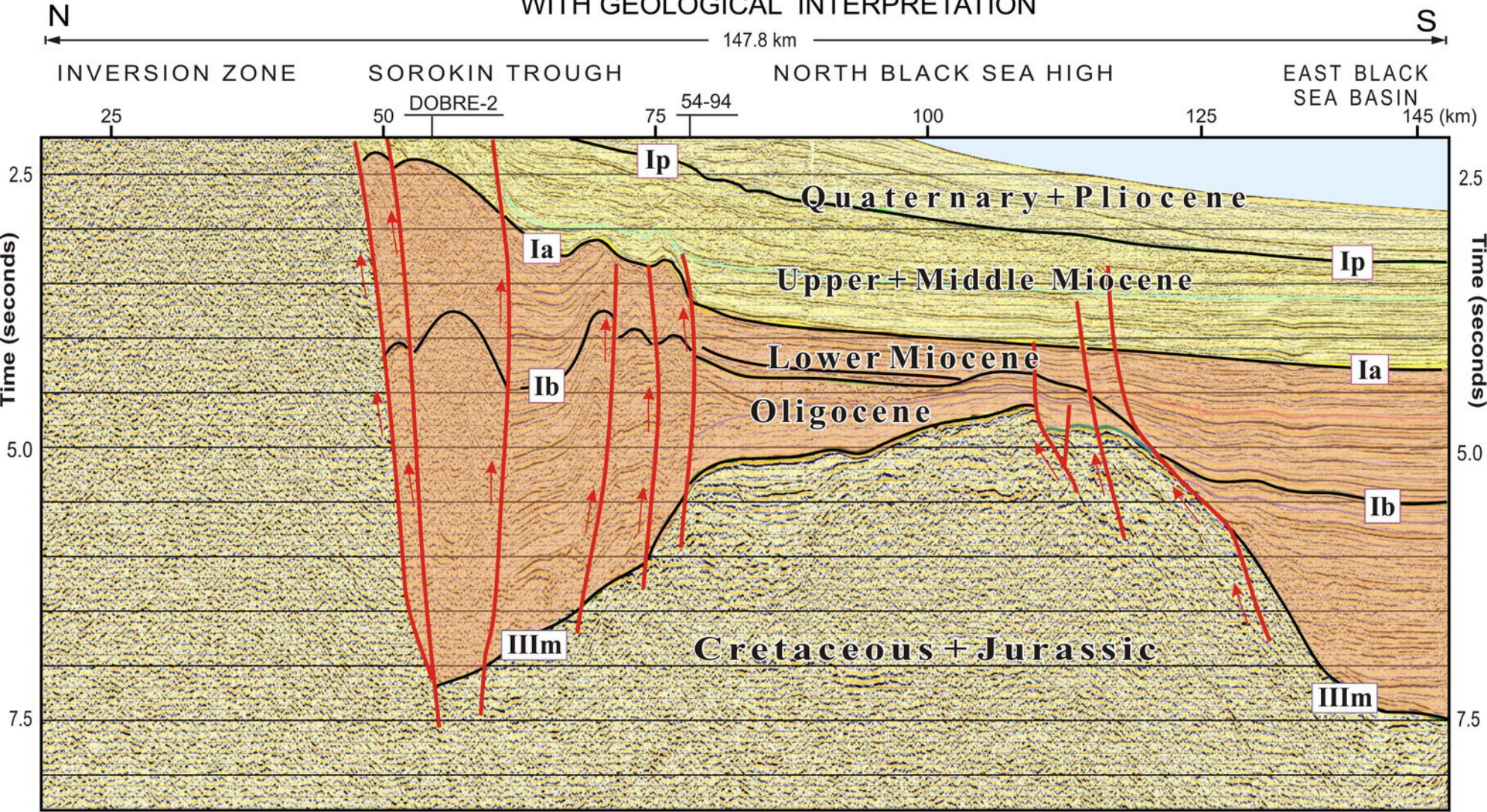


Fig. 4

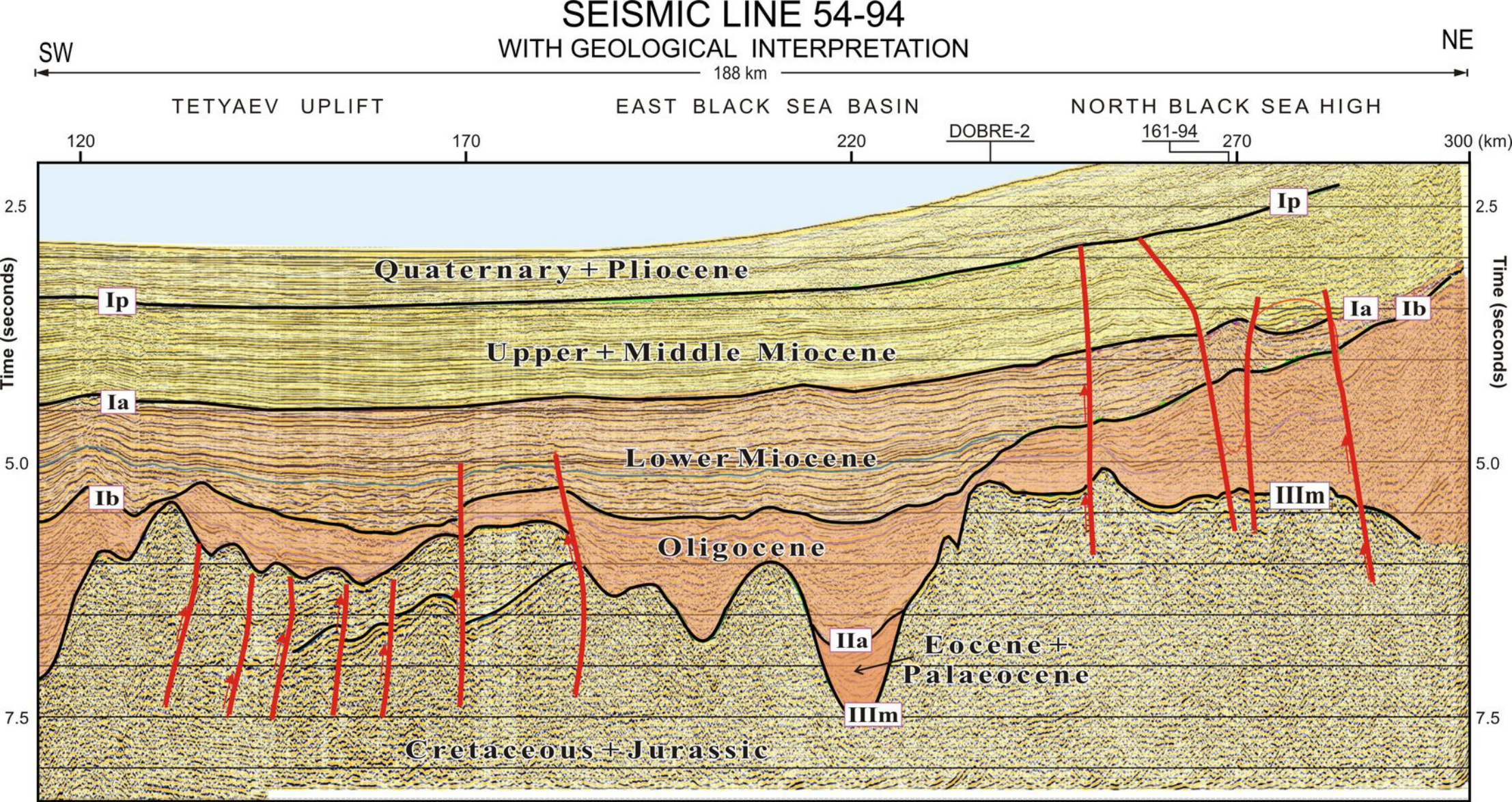


Fig. 5

REGIONAL SEISMIC LINE DOBRE-2 (BLACK SEA)

WITH GEOLOGICAL INTERPRETATION

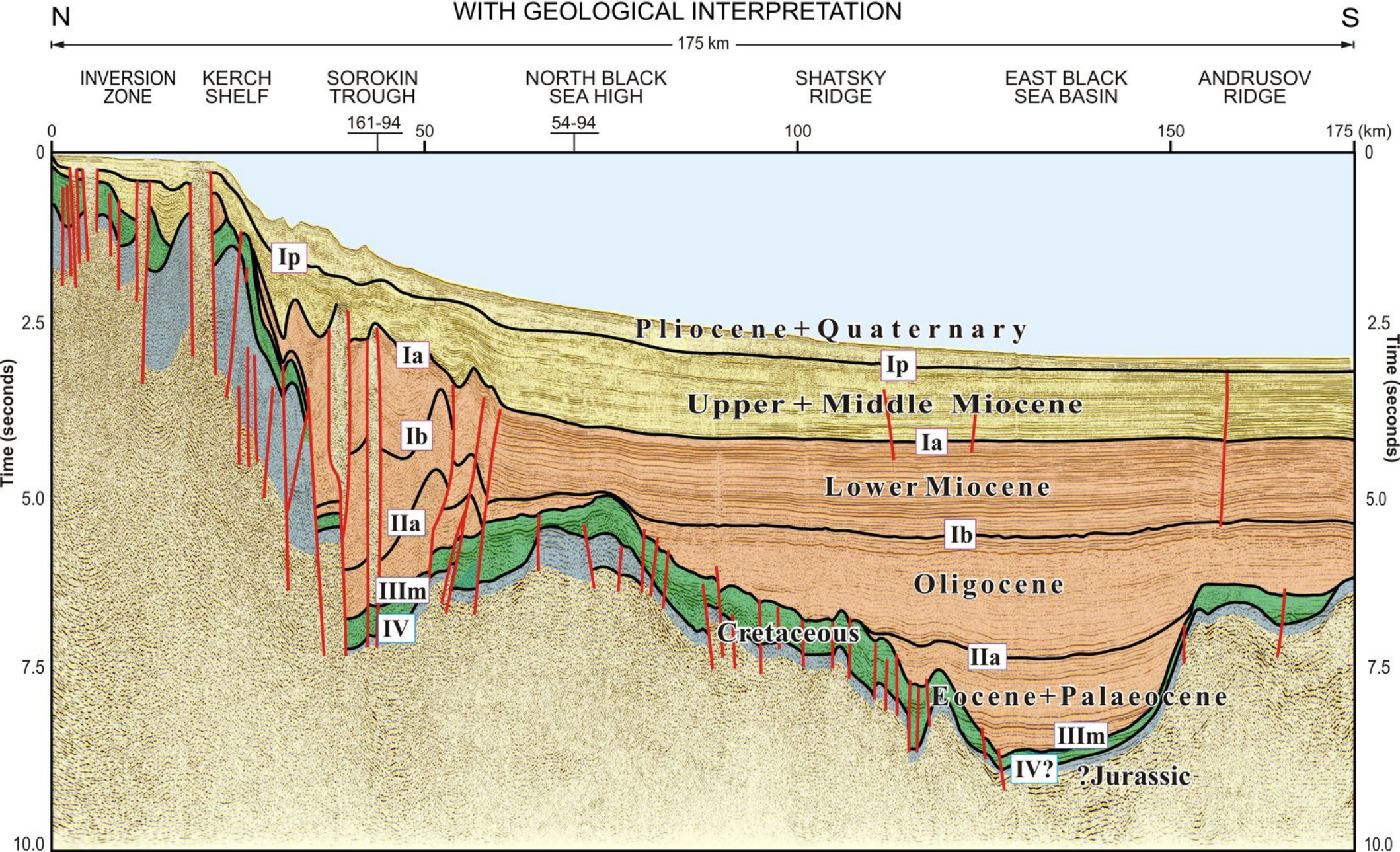


Fig. 6

